Trichostatin A inhibits proliferation of PC3 prostate cancer cells by disrupting the EGFR pathway

HONG ZHANG[1], XIN ZHAO[1], HONGBO LIU[1], HUI JIN[2] and YOUBO JI[2]

[1]Department of Clinical Medicine, Changchun Medical College, Changchun, Jilin 130031;
[2]Department of Pain Medical Center, The Second Hospital of Jilin University, Changchun, Jilin 130041, P.R. China

Abstract. Prostate cancer (PC) is the most common type of malignancy to exist in men within developed countries. Androgen deprivation therapy is performed for metastatic and advanced PC. However, the majority of cases of prostate cancer become refractory during therapy, leading to castration-resistant PC (CRPC). Histone deacetylases (HDACs) are key factors in regulating gene transcription and have been associated with cancer development. In the present study the small molecule inhibitor trichostatin A (TSA), which targets HDACs, was demonstrated to inhibit the proliferation of CRPC PC3 cells by disrupting the epidermal growth factor receptor (EGFR)-STAT3 pathway. The expression of EGFR and STAT3 was downregulated following TSA treatment, and cell cycle arrest was induced by downregulating the expression of cyclin D1 and CDK6, and via retinoblastoma protein phosphorylation. Furthermore, the transcription of cyclin D1 and CDK6 was suppressed by TSA. Apoptosis of PC3 cells treated with TSA was also investigated, and it was revealed that TSA induced apoptosis by upregulating BAX and downregulating BCL-2. The combination of TSA with doxorubicin exerted a synergistic inhibitory effect on PC3 cell proliferation through the induction of apoptosis. The results of the present study revealed a promising epigenetic-based therapeutic strategy that could be implemented in cases of CRPC.

Introduction

Prostate cancer (PC) is the most frequently diagnosed type of cancer among men throughout the developed world (1). It originates from high-grade prostatic intra-epithelial neoplasia

Correspondence to: Mr. Youbo Ji, Department of Pain Medical Center, The Second Hospital of Jilin University, 218 Ziqiang Street, Changchun, Jilin 130041, P.R. China
E-mail: jiyb@jlu.edu.cn

and often progresses to metastatic PC. Commonly, androgen deprivation therapy is the first-line treatment for patients with PC (2). However, most patients will relapse due to the development of castration-resistant PC (CRPC) after 2-3 years (3).

Previous evidence has suggested that the acquisition of androgen independence may be due to the upregulation of growth factor/receptor signaling pathways, principally that of the epidermal growth factor receptor (EGFR) (4,5), which is an attractive target for therapeutic intervention. EGFR is a multifunctional membrane glycoprotein expressed in numerous types of tissue (6). Furthermore, EGFR is overexpressed in many tumors, and leads to excessive cell proliferation and the development of malignancy (7). EGFR interacts with its ligand, EGF, to regulate cell growth, differentiation, motility, adhesion and tumorigenesis. EGF engagement activates the intrinsic kinase activity of EGFR, leading to the activation of several downstream intracellular signaling pathways, including those of MEK, ERK and PI3K/Akt, and STAT3 (8). STAT3 is activated by EGF and further regulates the expression of numerous genes involved in the cell cycle and proliferation, including cyclin D1, BCL-2 and surviving (9,10). Previous studies have demonstrated that constitutively activated STAT proteins are present in numerous types of tumor cells and cancer tissues, and that STAT3 is the most active transcription factor (11,12). Inhibition of EGFR inhibits these signaling cascades and further promotes apoptosis of cancer cells (13).

Epigenetic mechanisms, such as DNA methylation and histone modification, have important roles in cancer development. Histone deacetylases (HDACs), enzymes involved in removing acetyl groups from histones, remodel chromatin and regulate gene transcription, thereby serving crucial roles in cell proliferation, cell cycle regulation and cell differentiation (14,15). HDACs are overexpressed in a number of types of tumor (16,17), which indicates that HDACs may be potential targets for epigenetic intervention. Trichostatin A (TSA), a class I and II HDAC inhibitor, exerts anti-tumor effects in colon carcinoma, breast adenocarcinoma and esophageal squamous cells (18-20). Zhang *et al* (21) revealed that higher dosages of TSA (5-40 μM) exert potent activity against prostate cancer cells through the induction of cell cycle arrest and apoptosis.

In the present study, the anti-proliferative effect of a lower concentration of TSA (<1 μM) on PC3 cells was investigated as well as the potential of combination treatment with doxorubicin (DOX) in CRPC.

Materials and methods

Reagents. TSA and MG132 were purchased from Sigma-Aldrich (Merck KGaA). Stock solutions of TSA (2 mM) and MG132 (10 mM) were prepared using dimethyl sulfoxide (DMSO). The final concentration of DMSO in the medium was maintained at 0.1%. MG132, proteasome inhibitor was used to determine if decreased EGFR expression by TSA treatment was via proteasomal degradation.

Cell lines and culture. PC3 human prostate cancer cells from American Type Culture Collection were cultured in RPMI-1640 medium (Gibco; Thermo Fisher Scientific, Inc.) supplemented with 10% fetal bovine serum (HyClone; GE Healthcare Life Sciences) and penicillin (100 U/ml)/streptomycin (100 μg/ml), and were maintained at 37°C in a humidified atmosphere containing 5% CO_2.

MTT assay. A total of 3,000 cells in the logarithmic growth phase were seeded into 96-well plates. After 24 h of incubation, the cells were exposed to a range of concentrations (0-1 μM) of TSA and incubated for 72 h. After this, 10 μl MTT (5 mg/ml) solution was added to each well and incubated for 4 h at 37°C and 5% CO_2. Following incubation, the supernatant was removed, and the cells were suspended in 100 μl of 100% DMSO. The absorbance values were measured at 570 nm and were normalized to the DMSO control by using a Thermo Multiskan spectrum plate reader (Thermo Fisher Scientific, Inc.). The experiments were conducted in triplicate. The status of the cells in each group was evaluated at x100 magnification using a light microscope (CKX41; Olympus Corporation).

Cell cycle assay. Cells were treated with 0.5 μM TSA or the DMSO control for 24 h. Cells were then harvested and fixed in 70% cold ethanol at -20°C overnight. Cells were washed with 1X PBS and incubated with RNase at 37°C for 30 min, followed by propidium iodide (PI; 50 μg/ml) staining for another 30 min at 4°C. Cell suspensions were analyzed with a BD FACSCalibur™ flow cytometer (BD Biosciences). Data were analyzed with ModFit LT software (version 3.3; Verity Software House, Inc.).

Immunoblotting. PC3 cells were treated with TSA or combined with MG132 or doxorubicin for 24 h. Since EGF usually induces phosphorylation of EGFR within 30 min, phosphorylation of EGFR was determined at 10 min after EGF induction in PC3 cells treated with TSA for 30 min prior to EGF induction. After treatment, cells were washed with cold PBS and disrupted with 1X cell lysis buffer (Cell Signaling Technology, Inc.), followed by brief sonication (amplitude 20%, duration 3 sec, twice, on ice). The protein concentration was analyzed using a Bio-Rad protein assay kit II with bovine serum albumin standards, according to the manufacturer's protocol (cat. no. 5000002; Bio-Rad Laboratories, Inc.). Cell lysates were separated by SDS-PAGE (30 μg protein each lane; 10% gel for high or middle molecular weight and 15% gel for low molecular weight protein) and then transferred onto nitrocellulose membranes (Hybond-C; Amersham Pharmacia Biotech, Inc.). Following blocking with PBS-Tween-20 containing 5% non-fat dried milk for 1 h at room temperature, the membranes were incubated with primary antibodies against EGFR (1:1,000; cat. no. 2646), phospho-EGFR (1:1,000; cat. no. 4407), CDK6 (1:1,000; cat. no. 13331), CDK4 (1:1,000; cat. no. 12790), phospho-retinoblastoma (RB) protein (1:1,000; cat. no. 3590), RB (1:1,000; cat. no. 9309), BAX (1:1,000; cat. no. 5023), BCL-2 (1:1,000; cat. no. 2876), cleaved caspase-3 (1:1,000; cat. no. 9664) (all Cell Signaling Technology, Inc.), STAT3 (1:2,000; cat. no. ab68153), Cyclin D1 (1:1,000; cat. no. ab134175) and BCL-XL (1:1,000; cat. no. ab32370) (all from Abcam; overnight at 4°C. A horseradish peroxidase-conjugated secondary antibody (1:1,000; cat. no. 7074 or 7076; Cell Signaling Technology, Inc.) was then incubated with the membranes for 1 h at room temperature. Immunoreactivity bands were detected using an enhanced chemiluminescence kit (cat. no. NCI4106; Pierce; Thermo Fisher Scientific, Inc.). β-actin (1:1,000; cat. no. 3700; Cell Signaling Technology, Inc.) was used as the loading control.

Reverse transcription-quantitative (RT-qPCR). Total RNA was extracted from the PC3 cells treated with TSA with TRIzol® (Invitrogen; Thermo Fisher Scientific, Inc.), according to the manufacturer's protocol. cDNA was synthesized from 4 μg total RNA with Oligo (dT)$_{18}$ primer using the EasyScript first-strand cDNA synthesis superMix (TransGen Biotech Co., Ltd.) and ARKTIK Thermal Cycler (Thermo Fisher Scientific, Inc.), according to the manufacturer's protocol. The temperature protocol was as follows: Denaturation, 65°C for 5 min; annealing, on ice for 2 min; elongation, 42°C for 30 min; and termination, 85°C for 5 sec. PCR amplification, using 4 μl cDNA with TransStart® Green qPCR SuperMix (TransGen Biotech Co., Ltd.), for CDK6 and cyclin D1 genes was performed with the Mx3005p Real-Time PCR system (Agilent Technologies, Inc.) at 94°C for initial denaturation for 30 sec, followed by 40 cycles at 94°C for 6 sec and 60°C for 30 sec. The primer sequences were: CDK6 forward, 5'-CATTCAAAA TCTGCCCAACC-3' and reverse, 5'-GGTCCTGGAAGTATG GGTGA-3'; cyclin D1 forward, 5'-GCTTCCTCTCCAGAG TGATC-3' and reverse, 5'-GTCCATGTTCTGCTGGGCCT-3'. GAPDH forward, 5'-GTGAAGGTCGGAGTCAACGG-3' and reverse, 5'-CCTGGAAGATGGTGATGGGA-3'. GAPDH was used as the reference gene. Gene expression was calculated using the $2^{-\Delta\Delta Cq}$ method (22).

Statistical analysis. SPSS (version 21; IBM Corp.) software was used to perform the statistical analysis. Data are presented as the mean ± SD, with a minimum of 3 repeats. A Student's t-test (two-tailed) was used to compare between two groups. One-way analysis of variance was performed to compare multiple groups followed by Tukey's test to determine multiple comparisons between the groups. P<0.05 was considered to indicate a statistically significant difference.

Results

TSA inhibits PC3 cells by inactivating the EGFR. To evaluate the cytotoxic effect of TSA, the inhibitory effect of TSA on the proliferation of PC3 cells was investigated using an MTT assay. TSA inhibited PC3 cell proliferation in a dose- and time-dependent manner (Fig. 1A and B). Following treatment with 0.5 and 1.0 μM TSA for 72 h, the inhibitory rate was
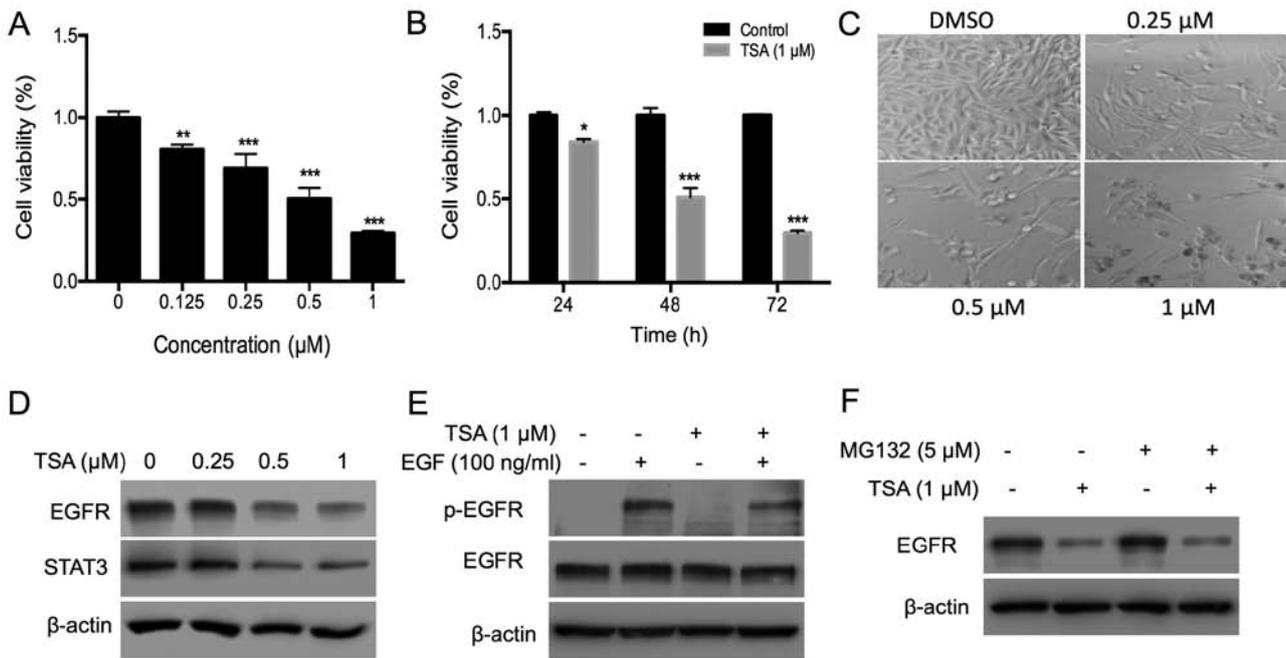
Figure 1. TSA inhibits PC3 cell proliferation by disrupting the EGFR-STAT3 pathway. (A) PC3 cells ($3x10^3$) were plated in a 96-well plate and treated with different doses of TSA (0, 0.25, 0.5 and 1 μM) for 72 h; an MTT assay was used to measure the effects of TSA on PC3 cell proliferation. (B) PC3 cells were subjected to the aforementioned treatments, and the time-course effect of TSA (1.0 μM) was measured using an MTT assay. (C) Effects of TSA on the density and morphology of PC3 cells were observed via microscopy. The magnification is x100. (D) Expression of EGFR and STAT3 in PC3 cells treated with TSA. PC3 cells ($4x10^5$) were plated in 6-cm dishes, and 0.25, 0.5 or 1 μM TSA was added for 24 h. DMSO was added into the control group wells. Cells were collected and lysed with lysis buffer and the protein expression analyzed via western blotting. (E) TSA inhibits the phosphorylation of EGFR induced by EGF. Cells were starved in serum-free medium for 12 h and then treated with 1 μM TSA for 30 min, followed by EGF (100 ng/ml) for 10 min. Cells were collected, and western blotting was used to evaluate the phosphorylation of EGFR. (F) Expression of EGFR in PC3 cells treated with TSA and MG132. Cells were treated with 1 μM TSA and 5 μM MG132 for 24 h. Cells were collected, and western blotting was used to evaluate the expression of EGFR. *P<0.05; **P<0.01; ***P<0.001 vs. respective control. TSA, trichostatin A; EGFR, epidermal growth factor; p, phosphorylated; DMSO, dimethyl sulfoxide.

~50 and 72%, respectively. The suppressive effect of TSA on cell proliferation was further confirmed by microscopic observation. Treatment with TSA decreased cell density (Fig. 1C). EGFR was evaluated as it is overexpressed in prostate cancer and has an important role in prostate cancer progression (23). Treatment with TSA for 24 h decreased the expression of EGFR and its downstream molecule STAT3 (Fig. 1D). Activity of EGFR was further determined by analyzing the phosphorylation level of EGFR. Since EGF usually induces phosphorylation of EGFR within 30 min, phosphorylation of EGFR was determined at 10 min after EGF induction in PC3 cells treated with TSA for 30 min prior to EGF induction. The results of the present study indicated that TSA treatment for 30 min decreased EGFR phosphorylation, but not expression, indicating that TSA treatment decreased both the expression and activity of EGFR (Fig. 1E). Treatment with HDAC inhibitors can induce ubiquitination and proteasomal degradation of the erbB family in head and neck squamous tumors (24). To test whether TSA suppressed EGFR expression in a proteasomal pathway, PC3 cells were treated with the proteasome inhibitor MG132. However, EGFR protein levels remained suppressed by TSA in the presence of MG132 (Fig. 1F), indicating that proteasomal degradation is not involved in the TSA-induced EGFR turnover.

TSA induces cell cycle arrest by downregulating the expression of CDK6 and cyclin D1, and the phosphorylation of RB. To identify the underlying mechanism associated with

the suppression of cell proliferation by TSA, cell cycle analysis was performed in the present study. The results revealed that treatment with TSA for 24 h led to an accumulation of PC3 cells in the G2/M phase (3.8 vs. 23.4%; P<0.01) and a concomitant decrease in the S-phase cell fraction (14.1 vs. 7%; P<0.01; Fig. 2A and B). TSA-induced cell cycle arrest was further confirmed by examining the expression of the cell cycle regulatory protein cyclin D1, CDK6, and the phosphorylation of RB in PC3 cells. Western blot analysis and RT-qPCR indicated that TSA treatment decreased cyclin D1 and CDK6 levels, and the phosphorylation of RB (Fig. 2C-E).

TSA induces apoptosis in PC3 cells. In addition to blocking the cell cycle phase transition, it has been demonstrated that TSA induces cell apoptosis in human breast cancer (18). To determine whether TSA induces apoptosis in prostate cancer cells, PC3 cells were treated with a TSA dose series for 24 h in the present study. The apoptotic percentage of PC3 cells following treatment was evaluated using flow cytometry. The sub-G1 fraction was markedly increased compared with the control (Fig. 3A and B). TSA-induced apoptosis was further confirmed by examining the expression of cleaved caspase-3 in PC3 cells. Western blot analysis indicated that TSA treatment increased cleaved caspase-3 in PC3 cells (Fig. 3C). Furthermore, BAX, BCL-2 and BCL-XL protein expression was measured in PC3 cells following TSA treatment. BAX protein was upregulated and BCL-2 protein was downregulated following treatment, while BCL-XL was not notably
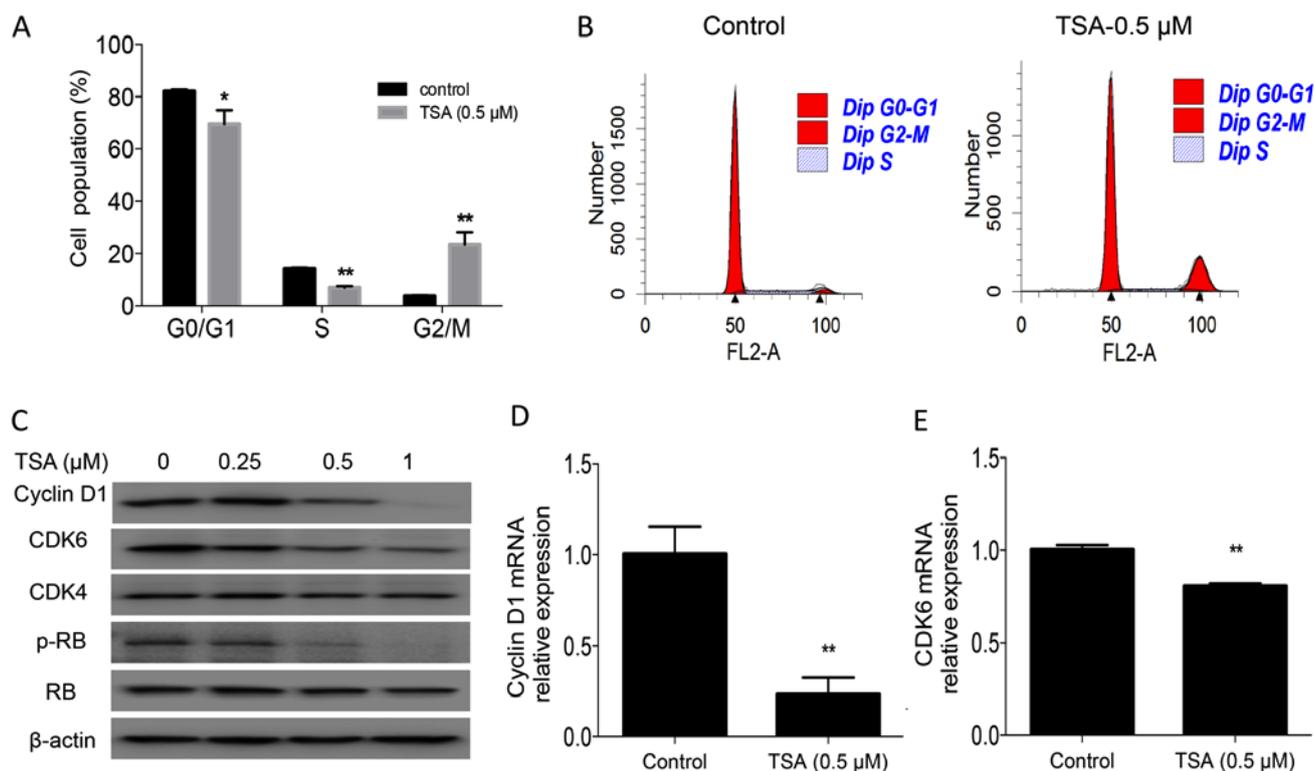
Figure 2. TSA induces G2/M phase cell cycle arrest in PC3 cells. (A) Cell cycle analysis was performed using PC3 cells. PC3 cells ($4x10^5$) were plated in 6-cm dishes and incubated overnight. Cells were treated with 0.5 μM TSA for 24 h. Cells were then harvested and fixed for analysis. (B) Representative histogram of cell cycle analysis using flow cytometry. (C) Expression of cyclin D1, CDK6, CDK4 and RB, and the phosphorylation of RB, was detected in PC3 cells treated with TSA for 24 h. (D) mRNA expression of cyclin D1 in PC3 cells treated with TSA for 24 h. PC3 cells were plated in 6-cm dishes and treated with TSA for 24 h. Cells were collected, and RNA was extracted using TRIzol®. Reverse transcription-quantitative PCR was conducted to detect the mRNA expression of cyclin D1. (E) mRNA expression of CDK6 in PC3 cells treated with TSA for 24 h, following the aforementioned protocol. *P<0.05; **P<0.01 vs. respective control. TSA, trichostatin A; RB, retinoblastoma protein; p, phosphorylated.

affected. These results indicated that TSA may induce PC3 apoptosis via the mitochondrial pathway.

TSA enhances apoptosis induced by DOX. The majority of cases of prostate cancer exhibit radio- and chemoresistance. In recent years, combinations of HDAC inhibitors with chemotherapy drugs have been used to treat various malignancies. In the present study the synergistic effect of TSA and DOX on the inhibition of PC3 cell proliferation was investigated. Notably, DOX and TSA in combination demonstrated consistent inhibitory effects on PC3 cells compared with either compound alone (Fig. 4A), as well as a clear elevation of cleaved caspase-3 (Fig. 4B; lanes 7 and 8), indicating a synergistic enhancement of PC3 cell apoptosis.

Discussion

The epigenetic regulation of gene expression may represent a potential new therapeutic strategy for cancer treatment. Histone acetylation is determined using histone acetyltransferases and HDACs. A variety of HDAC inhibitors have been demonstrated to induce apoptosis in solid tumors (18,21,25-27). In the present study, the effects of TSA, a potent HDAC inhibitor, on disrupting EGFR signaling were characterized, demonstrating the induction of apoptosis in prostate cancer cells. Molecular evidence for cell cycle arrest was provided in the decreased expression of cyclin D1 and CDK6, and the decreased

phosphorylation of RB, in addition to the increased levels of BAX and decreased levels of BCL-2. Notably, blocking the EGFR signaling pathway sensitized PC3 cells to DOX.

HDAC inhibitors exert transcriptional repression of certain oncogenes, such as MYC, MYCN and EGFR (28-30). In the present study, it was demonstrated that TSA treatment led to downregulated EGFR and STAT3 expression, resulting in decreased cyclin D1 and CDK6 expression, and thus G2/M cell cycle arrest, which is in accordance with the results of the aforementioned studies. These results are, however, different to previous conclusions (21) that higher concentrations of TSA induce both G0/G1 and G2/M arrest in PC3 cells, which indicates that the biological function of TSA is dose-dependent. In addition to blocking cell cycle progression, HDAC inhibitors induce apoptosis via the mitochondria-mediated apoptosis pathway (25), which disrupts the ratio of BAX to BCL-2 or BCL-XL at the mitochondrial membrane, causing the release of cytochrome c and other pro-apoptotic molecules into the cytoplasm, which in turn leads to the activation of caspase-3 to cleave poly (ADP-ribose) polymerase and execute cell death. In the present study, the sub-G1 fraction in the cell cycle analysis was determined to represent apoptosis induction by TSA. This method is an older technique used for the detection of apoptosis, which could be replaced by Annexin V and PI double staining to distinguish apoptotic and necrotic cells. In order to demonstrate the inducible role of TSA in apoptosis, the level of cleaved caspase-3 was determined using
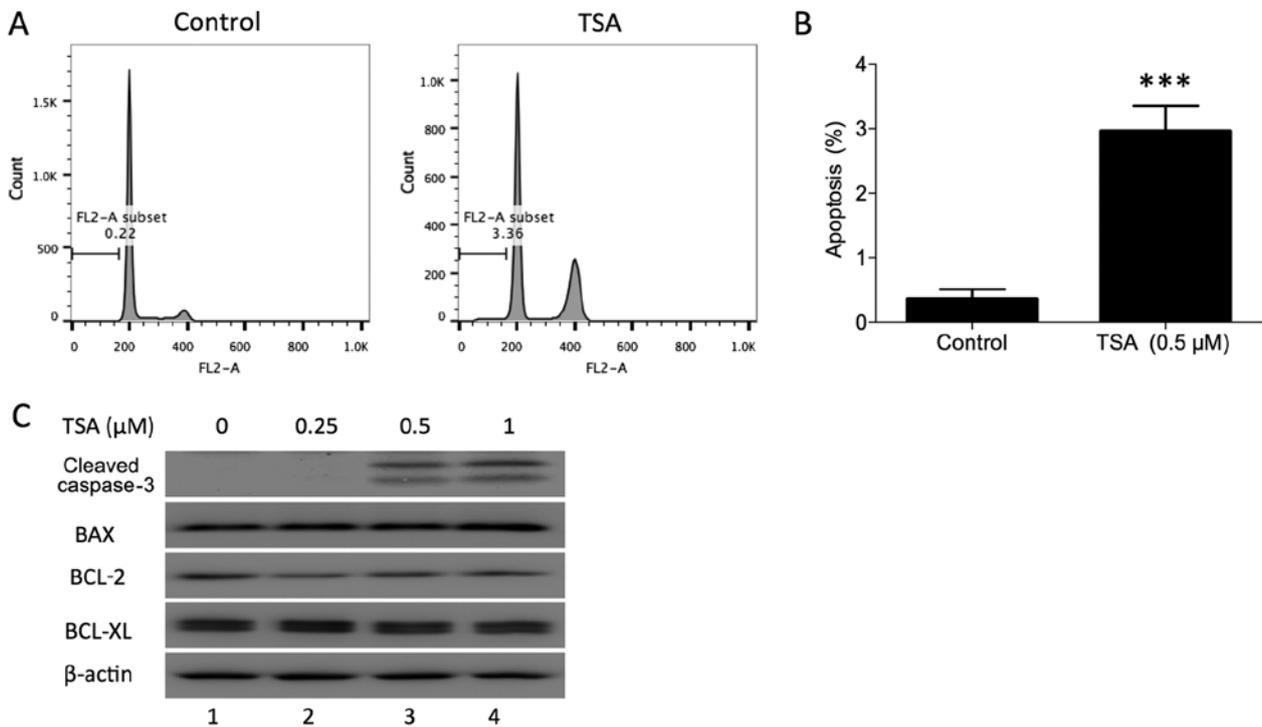
Figure 3. TSA induces apoptosis in PC3 cells. (A) Representative histogram of apoptosis induced by TSA in PC3 cells. (B) Proportion of apoptotic PC3 cells following treatment with TSA. ***P<0.001 vs. control. (C) PC3 cells were treated with different doses of TSA (0, 0.25, 0.5 and 1 μM), and then collected 24 h after treatment. Cleaved caspase-3, BAX, BCL-2 and BCL-XL were detected using Western blotting. TSA, trichostatin A.
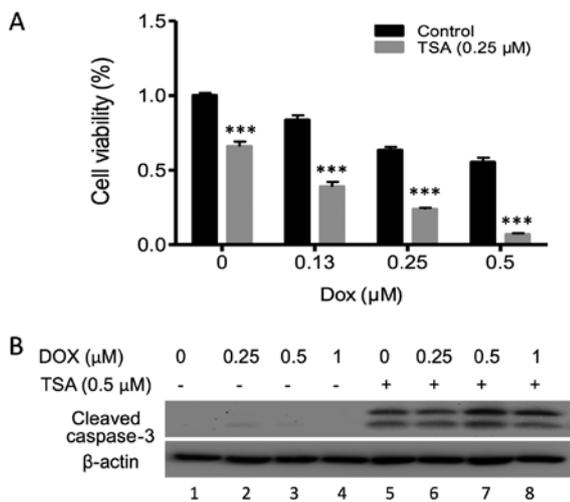

Figure 4. Synergistic inhibitory effects exerted by the TSA and DOX combination on PC3 cell proliferation by inducing cell apoptosis. (A) An MTT assay was performed to assess the synergistic effects of TSA and DOX on the proliferation of PC3 cells. PC3 cells were treated with 0.25 μM TSA and different doses of DOX (0, 0.13, 0.25 or 0.5 μM) for 72 h. ***P<0.001 vs. respective control. (B) PC3 cells were treated with TSA and DOX, and cleaved caspase-3 was detected 24 h after treatment in PC3 cells. TSA, trichostatin A; DOX, doxorubicin.

western blot analysis, which is a common character of apoptosis. It was revealed that TSA increased cleaved caspase-3 expression, confirming the induction of apoptosis. Consistent with a previous study, the present study demonstrated that TSA decreased BCL-2 expression (21). Furthermore, it was revealed that TSA treatment increased BAX expression, thereby activating the mitochondria-mediated apoptosis pathway (31). Blocking cell cycle progression and inducing apoptosis is a common mechanism of chemotherapeutic agents to exert anti-proliferative effects. Consistent with a previous study, TSA treatment led to simultaneous cell cycle arrest and apoptosis (21).

DOX is an anthracycline antibiotic that is effective in treating a wide range of different types of cancer (32). However, the toxic side effects of DOX, particularly those involving cardiac damage, limit its clinical application for long-term therapy (33). Drug combinations are a widely used strategy to increase the efficacy and decrease the side effects of chemotherapy. Herein, the combination of TSA and low-dose DOX exerted synergistic effects in reducing PC3 cell viability. Higher levels of cleaved caspase-3 were induced by this combination, and indicated that TSA could promote cell apoptosis induced by DOX (34).

In conclusion, the HDAC inhibitor TSA induced cell cycle arrest and apoptosis in PC3 cells by inactivating the EGFR-STAT3 signaling pathway. When combined, TSA and DOX exert synergistic effects in reducing PC3 cell viability by promoting apoptosis. Although TSA is an epigenetic regulator, the present study did not establish a mechanistic association between TSA and the epigenetic regulation of gene expression in PC3 cells. Another limitation of the present study is that only the single cell line PC3 was used to evaluate TSA effect. Further studies are required to determine how TSA blocks the EGFR pathway in an epigenetic manner using multiple cell lines, including DU145 and LNcap. The present study supports the rationale for TSA alone or in combination with DOX as a therapeutic approach to CRPC cases, which are largely refractory to current therapeutic approaches, and may promote the rapid clinical evaluation of this strategy.

Availability of data and materials

All data generated or analyzed during this study are included in this published article.

Authors' contributions

HZ, XZ, HL, HJ and YJ conceived, designed and performed the experiments and analyzed the data. HZ, XZ, HL and HJ contributed to the reagents and/or materials used in the present study. HZ and YJ wrote the manuscript. All authors confirm the accuracy of the study.

Ethics approval and consent to participate

Not applicable.

Patient consent for publication

Not applicable.

Competing interests

The authors declare that they have no competing interests.

References

1. Kgatle MM, Kalla AA, Islam MM, Sathekge M and Moorad R: Prostate cancer: Epigenetic alterations, risk factors, and therapy. Prostate Cancer 2016: 5653862, 2016.
2. Liu C, Zhu Y, Lou W, Nadiminty N, Chen X, Zhou Q, Shi XB, deVere White RW and Gao AC: Functional p53 determines docetaxel sensitivity in prostate cancer cells. Prostate 73: 418-427, 2013.
3. Grasso CS, Wu YM, Robinson DR, Cao X, Dhanasekaran SM, Khan AP, Quist MJ, Jing X, Lonigro RJ, Brenner JC, *et al*: The mutational landscape of lethal castration-resistant prostate cancer. Nature 487: 239-243, 2012.
4. Traish AM and Morgentaler A: Epidermal growth factor receptor expression escapes androgen regulation in prostate cancer: A potential molecular switch for tumour growth. Br J Cancer 101: 1949-1956, 2009.
5. Kambhampati S, Ray G, Sengupta K, Reddy VP, Banerjee SK and Van Veldhuizen PJ: Growth factors involved in prostate carcinogenesis. Front Biosci 10: 1355-1367, 2005.
6. Tzouvelekis A, Ntolios P, Karameris A, Vilaras G, Boglou P, Koulelidis A, Archontogeorgis K, Kaltsas K, Zacharis G, Sarikloglou E, *et al*: Increased expression of epidermal growth factor receptor (EGF-R) in patients with different forms of lung fibrosis. Biomed Res Int 2013: 654354, 2013.
7. Liu YH, Wei XL, Hu GQ and Wang TX: Quinolone-indolone conjugate induces apoptosis by inhibiting the EGFR-STAT3-HK2 pathway in human cancer cells. Mol Med Rep 12: 2749-2756, 2015.
8. Wee P and Wang Z: Epidermal growth factor receptor cell proliferation signaling pathways. Cancers (Basel) 9: 52, 2017.
9. Weerasinghe P, Garcia GE, Zhu Q, Yuan P, Feng L, Mao L and Jing N: Inhibition of Stat3 activation and tumor growth suppression of non-small cell lung cancer by G-quartet oligonucleotides. Int J Oncol 31: 129-136, 2007.
10. Zhang X, Yue P, Page BD, Li T, Zhao W, Namanja AT, Paladino D, Zhao J, Chen Y, Gunning PT and Turkson J: Orally bioavailable small-molecule inhibitor of transcription factor Stat3 regresses human breast and lung cancer xenografts. Proc Natl Acad Sci USA 109: 9623-9628, 2012.
11. Tai WT, Cheng AL, Shiau CW, Huang HP, Huang JW, Chen PJ and Chen KF: Signal transducer and activator of transcription 3 is a major kinase-independent target of sorafenib in hepatocellular carcinoma. J Hepatol 55: 1041-1048, 2011.
12. Kortylewski M and Yu H: Stat3 as a potential target for cancer immunotherapy. J Immunother 30: 131-139, 2007.
13. Su JC, Lin KL, Chien CM, Chuang PW, Chang LS and Lin SR: Concomitant inactivation of the epidermal growth factor receptor, phosphatidylinositol 3-kinase/Akt and Janus tyrosine kinase 2/signal transducer and activator of transcription 3 signalling pathways in cardiotoxin III-treated A549 cells. Clin Exp Pharmacol Physiol 37: 833-840, 2010.
14. Minucci S and Pelicci PG: Histone deacetylase inhibitors and the promise of epigenetic (and more) treatments for cancer. Nat Rev Cancer 6: 38-51, 2006.
15. Reichert N, Choukrallah MA and Matthias P: Multiple roles of class I HDACs in proliferation, differentiation, and development. Cell Mol Life Sci 69: 2173-2187, 2012.
16. Kwiecińska P, Wróbel A, Taubøll E and Gregoraszczuk EŁ: Valproic acid, but not levetiracetam, selectively decreases HDAC7 and HDAC2 expression in human ovarian cancer cells. Toxicol Lett 224: 225-232, 2014.
17. Weichert W, Röske A, Gekeler V, Beckers T, Stephan C, Jung K, Fritzsche FR, Niesporek S, Denkert C, Dietel M and Kristiansen G: Histone deacetylases 1, 2 and 3 are highly expressed in prostate cancer and HDAC2 expression is associated with shorter PSA relapse time after radical prostatectomy. Br J Cancer 98: 604-610, 2008.
18. Sun S, Han Y, Liu J, Fang Y, Tian Y, Zhou J, Ma D and Wu P: Trichostatin A targets the mitochondrial respiratory chain, increasing mitochondrial reactive oxygen species production to trigger apoptosis in human breast cancer cells. PLoS One 9: e91610, 2014.
19. Watson JA, McKenna DJ, Maxwell P, Diamond J, Arthur K, McKelvey-Martin VJ and Hamilton PW: Hyperacetylation in prostate cancer induces cell cycle aberrations, chromatin reorganization and altered gene expression profiles. J Cell Mol Med 14: 1668-1682, 2010.
20. Ma J, Guo X, Zhang S, Liu H, Lu J, Dong Z, Liu K and Ming L: Trichostatin A, a histone deacetylase inhibitor, suppresses proliferation and promotes apoptosis of esophageal squamous cell lines. Mol Med Rep 11: 4525-4531, 2015.
21. Zhang Y, Xu Q, Liu G, Huang H, Lin W, Huang Y, Chi Z, Chen S, Lan K, Lin J and Zhang Y: Effect of histone deacetylase on prostate carcinoma. Int J Clin Exp Pathol 8: 15030-15034, 2015.
22. Livak KJ and Schmittgen TD: Analysis of relative gene expression data using real-time quantitative PCR and the 2(-Delta Delta C(T)) method. Methods 25: 402-408, 2001.
23. Gan Y, Shi C, Inge L, Hibner M, Balducci J and Huang Y: Differential roles of ERK and Akt pathways in regulation of EGFR-mediated signaling and motility in prostate cancer cells. Oncogene 29: 4947-4958, 2010.
24. Bruzzese F, Leone A, Rocco M, Carbone C, Piro G, Caraglia M, Di Gennaro E and Budillon A: HDAC inhibitor vorinostat enhances the antitumor effect of gefitinib in squamous cell carcinoma of head and neck by modulating ErbB receptor expression and reverting EMT. J Cell Physiol 226: 2378-2390, 2011.
25. You BR and Park WH: Trichostatin A induces apoptotic cell death of HeLa cells in a Bcl-2 and oxidative stress-dependent manner. Int J Oncol 42: 359-366, 2013.
26. Frew AJ, Johnstone RW and Bolden JE: Enhancing the apoptotic and therapeutic effects of HDAC inhibitors. Cancer Lett 280: 125-133, 2009.
27. Emanuele S, Lauricella M, Carlisi D, Vassallo B, D'Anneo A, Di Fazio P, Vento R and Tesoriere G: SAHA induces apoptosis in hepatoma cells and synergistically interacts with the proteasome inhibitor Bortezomib. Apoptosis 12: 1327-1338, 2007.
28. Chou CW, Wu MS, Huang WC and Chen CC: HDAC inhibition decreases the expression of EGFR in colorectal cancer cells. PLoS One 6: e18087, 2011.
29. LaBonte MJ, Wilson PM, Fazzone W, Russell J, Louie SG, El-Khoueiry A, Lenz HJ and Ladner RD: The dual EGFR/HER2 inhibitor lapatinib synergistically enhances the antitumor activity of the histone deacetylase inhibitor panobinostat in colorectal cancer models. Cancer Res 71: 3635-3648, 2011.

30. Yokoyama S, Feige E, Poling LL, Levy C, Widlund HR, Khaled M, Kung AL and Fisher DE: Pharmacologic suppression of MITF expression via HDAC inhibitors in the melanocyte lineage. Pigment Cell Melanoma Res 21: 457-463, 2008.
31. Kiliccioglu I, Konac E, Varol N, Gurocak S and Yucel Bilen C: Apoptotic effects of proteasome and histone deacetylase inhibitors in prostate cancer cell lines. Genet Mol Res 13: 3721-3731, 2014.
32. Lou Y, Wang Z, Xu Y, Zhou P, Cao J, Li Y, Chen Y, Sun J and Fu L: Resveratrol prevents doxorubicin-induced cardiotoxicity in H9c2 cells through the inhibition of endoplasmic reticulum stress and the activation of the Sirt1 pathway. Int J Mol Med 36: 873-880, 2015.
33. Menna P, Paz OG, Chello M, Covino E, Salvatorelli E and Minotti G: Anthracycline cardiotoxicity. Expert Opin Drug Saf 11 (Suppl 1): S21-S36, 2012.
34. Wang X, Xu J, Wang H, Wu L, Yuan W, Du J and Cai S: Trichostatin A, a histone deacetylase inhibitor, reverses epithelial-mesenchymal transition in colorectal cancer SW480 and prostate cancer PC3 cells. Biochem Biophys Res Commun 456: 320-326, 2015.